

# Evaluation of Major Factors Affecting Spatial Resolution of Gamma-Rays Camera

Hongwei Xie<sup>1</sup>, Jinchuan Chen<sup>1</sup>, Qiang Yi<sup>1</sup>, Faqiang Zhang<sup>1</sup>, Linbo Li<sup>1</sup>

<sup>1</sup>Institute of Nuclear Physics and Chemistry, China Academy of Engineering Physics, Mianyang, Sichuan, P.R. China, 621900

## Abstract

*Gamma-rays camera is mainly used in image diagnostics of intense pulse radiation sources<sup>[1]</sup>. The spatial resolution of the camera was measured on a <sup>60</sup>Co gamma-rays source with edge method. The spatial resolution MTF (modulation transfer function) at the 10% intensity was about 2 lp/mm and the maximal single-noise ratio (SNR) of the camera was found to be about 5:1. In addition, the spatial resolution of the camera was measured with pulse X-rays with 0.3 MeV in average energy and exclusion of effects of secondary electrons from consideration. Accordingly, the spatial resolution MTF at the 10% intensity was about 5lp/mm, verifying effects of secondary electrons induced by 1.25MeV gamma-rays in the scintillator upon the spatial resolution. Based on our analysis, dispersion sizes of secondary electrons in the scintillator are about 0.4 mm–0.6 mm. Comparatively, as indicated by detailed analysis of spatial resolutions of the MCP image intensifier and CCD devices, both have little effect on the camera's spatial resolution and could be well neglected.*

## 1 Introduction

A  $\gamma$ -rays camera was developed for the image diagnostics of intense pulsed  $\gamma$ -rays radiation sources, which consisted of rays-fluorescence convertor, optical imaging system, MCP+CCD, electronic control system and other devices. Due to its good performances in various adjustable parameters including exposure time spot, exposure time duration and gain, the camera has been widely used in the framing image diagnostics of pulse radiation fields<sup>[1,2]</sup>.

Point spread function (PSF) of the image diagnostic system is not only a major technical specification of a imaging system performances, but also a major factor to cause image degradation. A given PSF could be considered as a major criteria for the uncertainty evaluation of a given image and for the image super-resolution reconstruction. Other parameters to describe system spatial resolution include modulation transfer function (MTF) and linear spread function (LSF). The integration of PSF along 1-D direction would provide LSF, which would then provide MTF after Furrier Transform. All three parameters (PSF, LSF and MTF) could reflect the spatial resolution of the rays system<sup>[3]</sup>.

Edge method is a common method for the measurement of spatial resolution of  $\gamma$ -rays cameras<sup>[3]</sup>. An edge would be placed in 2°-3° angle with the pixel array to minimize effects of sub-pixels upon the spatial resolution, and the data would be fitted to curves to provide a very smooth measurement data. However, in dealing with the spatial resolution measurement of  $\gamma$ -rays cameras with thick scintillator and/or high energy, such a data processing might be technically difficult in various aspects<sup>[4]</sup>: 1) big detective quantum efficiency (DQE) fluctuations induced by interactions between high energy  $\gamma$ -rays and scintillator; 2) relatively big quantum gain of the  $\gamma$ -rays-fluorescence convertor; 3) relatively

more measurement steps. Another important factor to affect the spatial resolution is the measurement condition. Presumably, an ideal parallel radiation source with angular distribution would be most desirable for the measurement. However, the measurement of the spatial resolution would inevitably be affected by various factors: the size of the radiation source, the system structure, working conditions of the system, etc. Moreover, data processing from edge spread function (ESF) to LSF and then to MTF or PSF would also amplify noise. All factors add up to lead a relatively big uncertainty in the spatial resolution of the high energy  $\gamma$ -rays camera. In order to contain DQE effects in measurement results, serial procedures are applied.

The geometrical spatial resolution of the  $\gamma$ -rays camera is about 0.1mm/pixel. In order to provide a higher DQE, some special methods were introduced, e.g. to use an optical structure with short distance and a big field of view and to increase the scintillator, etc. The spatial resolution of the  $\gamma$ -rays camera was measured on a Co radiation source. And spatial resolutions of camera components were also studied respectively for the scintillator, MCP image intensifier, CCD camera, etc., to provide some valuable reference for further improvement of the spatial resolution of the  $\gamma$ -rays camera.

## 2 Experimental set up

### 2.1 Gamma-rays Camera

This camera is characterized in high sensitivity, high resolution and big dynamic range. The process could roughly be interpreted as follows. Firstly, the radiation source is imaged onto the imaging plane by  $\gamma$ -rays. Then the fluorescence image is imaged onto the incident plane of the MCP image intensifier through optical imaging system and conversion system. Finally, the intensified image is recorded by CCD device, while MCP and CCD are coupled with fiber plate. Major parts of the system are  $\gamma$ -rays imaging system and image recording system. A scintillator crystal(e.g., YAG, LSO, LYSO, etc.) is used to convert  $\gamma$ -rays into fluorescence image. A copper reflector with an efficiency of over 95% is placed in a 45° angle with  $\gamma$ -rays direction to reflect the fluorescence image, meanwhile to avoid direct  $\gamma$ -rays irradiation onto the MCP image intensifier and CCD camera. This specially developed imaging system could provide an amplification factor of 5:1 and a light collection efficiency of over 95%. The MCP image intensifier's spatial resolution is over 37 lp/mm. Besides, the intensifier is also characterized in tunable shutter time and electron gain, which could facilitate the imaging of  $\gamma$ -rays at different time. The amplification factor of the fiber plate is 1.5:1, providing a stable and reliable recording system. The CCD camera was provided by Andor Co. Ltd specifically for scientific purpose, with a pixel array of 1024×1024, pixel size of 13.3  $\mu\text{m}$ ×13.3  $\mu\text{m}$ . Moreover, the CCD could be used in a very low temperature even below -65 °C, making it a favorite option for imaging diagnostics

with low signal intensity. The total system is placed into an iron container to provide a sealed and shielded environment to avoid effects of electromagnetic effects.

## 2.2 Spatial Resolution Measurement with Edge Method

The experiment was carried out on the intense Co source in CAEP. The schematic experimental set-up is given in Figure 1. The  $^{60}\text{Co}$   $\gamma$ -rays source is a line source with a geometrical parameter of  $\Phi 11 \text{ mm} \times 450 \text{ mm}$ . It's intensity for every line is about  $10^4 \text{ Ci} = 3.7 \times 10^{14} \text{ Bq}$ . A  $5 \text{ mm} \times 50 \text{ mm}$  Pb slit gap (200 mm in thickness) was used for beam collimation and constraint. A 100 mm tungsten edge collimator was placed in front of but closely contacted with scintillator at the same time. The radiation flux of  $\gamma$ -rays at the scintillator was about  $9.0 \times 10^6 \text{ } \gamma/\text{cm}^2 \cdot \text{s}$ . As for the system collimation and adjustment, the procedure might be described as follows. Firstly, a laser beam with a diameter of 0.5mm was transmitted to traverse the front center and back center of the slit gap collimator. Then the beam would be irradiated onto the scintillator surface perpendicularly. Finally, the 100mm-thick tungsten edge would be placed parallel with the laser beam, and the edge image would be adjusted to be at the center of the field of view of the system. In addition, due to the high sensitivity of the MCP image intensifier and CCD devices to  $\gamma$ -rays, another 10cm-thick Pb shield was used to protect the system. After installation and adjustment, the radiographic system could be operated with PC remote control.

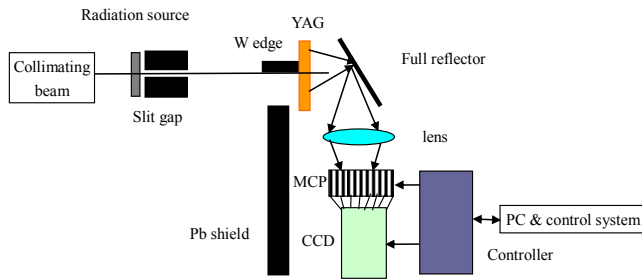


Fig. 1 The schematic diagram for the PSF measurement of the  $\gamma$ -rays camera

## 3 Experimental data and data processing

### 3.1 Performance Calibration of Radiographic System

Firstly, the flat field response is a major standard to evaluate the response uniformity of the radiographic system.  $\gamma$ -rays could presumably have a homogenous spatial distribution. Image signals corresponding to various radiation doses were experimentally calibrated. According to the result, flat field responses under various radiation doses were same, intensities in the central region were relatively high, and the non-homogeneities in the central region and edge region were about 30%. Flat field images are mainly used for the homogenous correction of radiographic images. After correction, images could convey information about the intensity distribution of incident  $\gamma$ -rays.

Secondly, the geometrical distortion of the radiographic system was also calibrated with black-and-white squares ( $5 \text{ mm} \times 5 \text{ mm}$  in

size). Image signals were obtained and analyzed with image processing programs. As indicated by results, the geometrical distortion of the radiographic system was in agreement with experimental requirements.

Finally, the dynamic sensitivity of the radiographic system was calibrated. Homogenous  $\gamma$ -rays were used to irradiate the scintillator, and radiation images corresponding to various radiation doses were recorded. After data processing, relationship curves between the radiation doses and image signal intensities could be well obtained. As indicated by these curves, with a radiation dose range of  $1.0 \times 10^6 \sim 2.0 \times 10^8$ , the radiographic system could demonstrate a fairly good linearity.

### 3.2 Experimental Data

The edge image experimentally obtained is given in Figure 2. Despite that a 100mm-thick W collimator was placed in region with relatively lower intensity to provide an attenuation factor of more than  $10^{-6}$ , the SNR of the system was found to be only 5:1. The major reason for this might be attributed to fluorescence dispersion effects throughout the fluorescence transmittance. Despite of the Pb shield, the scattered  $\gamma$ -rays along the optical path still acted as a non-negligible source to induce the noise.

Due to the relatively big non-homogeneity of the system, only an effective region  $100 \times 100$  in size was adopted for data processing. As shown in Figure 2, image signals fluctuated in relatively big amplitude with a standard deviation of about 3753, which might be attributed to single-particle detecting effects of the scintillator and relatively high quantum gains of the scintillator and MCP image intensifier, etc. Thus, during data processing, averaging was made for 100-line data, and the averaged data was subject to Gaussian fitting. Finally, ESF curves obtained could be very uniform and smooth (as shown in Figure 3).

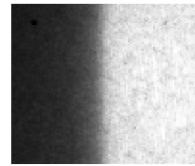


Fig.2 The experimentally obtained edge fluorescence image

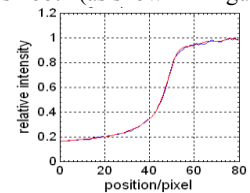


Fig. 3 The experimentally obtained ESF distribution

### 3.3 Spatial Distribution of System

Both MTF and PSF are important parameters to evaluate the spatial resolution of the radiographic system, but very difficult to be measured directly. However, they are functions of the LSF, while LSF could be determined by differentiating ESF obtained above:

$$LSF(x) = \frac{d[ESF(x)]}{dx} \quad (1)$$

MTF is the result of the Fourier Transform of LSF:

$$MTF(f) = \left| \frac{\int_{-\infty}^{\infty} LSF(x) \exp(-j2\pi fx) dx}{\int_{-\infty}^{\infty} LSF(x) dx} \right| \quad (2)$$

And the relationship between PSF and LSF could be given as follows:<sup>[4]</sup>

$$PSF(r) = -\frac{1}{\pi} \int_r^{\infty} \frac{d[LSF(x)]/dx}{(x^2 - r^2)^{1/2}} dx \quad (3)$$

Based on equations above, the LSF, MTF and PSF of the  $\gamma$ -rays camera could be obtained as given in Figure 4. As shown, with 10% intensity, the MTF is only 2 lp/mm, and the point spread size is about 2mm.

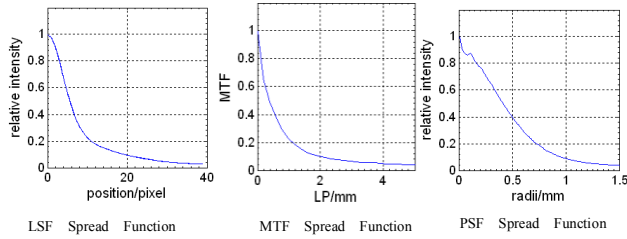


Fig. 4 The experimentally obtained LSF, MTF and PSF of the  $\gamma$ -rays camera

## 4 major factors affecting spatial resolution

The spatial resolution of the  $\gamma$ -rays camera was measured with edge method. In the following parts, effects of scintillator, MCP image intensifier and CCD camera upon the system spatial resolution will be analyzed, respectively.

### 4.1 PSF of CCD Device

The spatial resolution of CCD device is mainly dependent on the pixel size and the electron diffusion in the silica substrate. In the silica substrate, electron-hole pairs would be induced by photons. And electrons would spread in the substrate and move driven by the superposed voltage before stored in potential wells. The spread size or dimension of electrons in the silica substrate depends on the superposed voltage<sup>[6,9]</sup>. And that the superposed voltage is dependent on the substrate thickness and manufacturing process. With a superposed voltage ranging in 2.84 V~115.4 V, electron spread sizes are within 48.8 $\mu$ m to 3.7 $\mu$ m, and the electron spread function is basically in accordance with the Gaussian function distribution. The LSF of electrons could be described in the following equation<sup>[5]</sup>:

$$LSF(x) = a + b \cdot \exp\left(-\frac{(x - x_0)^2}{2\sigma^2}\right) \quad (4)$$

where:  $a$ ,  $b$ ,  $x_0$  and  $\sigma$  are fitting constants. The spread of electrons in the silica substrate could be obtained by using a point light source with a negligible size, sub-pixel sampling method and Gaussian function fitting<sup>[5, 6, 7]</sup>. In the high precision image

measurement, the electron spread in the silica substrate is a non-negligible factor to cause the degradation. Thus, in the common design of the scientific-level high sensitivity CCD, the back illumination method is used, and the thickness of the silica substrate is deliberately determined to be 10 $\mu$ m~15 $\mu$ m, which is roughly equal to electron spread sizes (5~10 $\mu$ m)<sup>[9]</sup>. The typical electron PSF is given in Figure 5, showing that the electron spread size is about 20 $\mu$ m corresponding to 10% intensity. Specifically, for a CCD with a pixel size of 13.3 $\mu$ m $\times$ 13.3 $\mu$ m, the electron spread might be about 1 to 2 pixels.

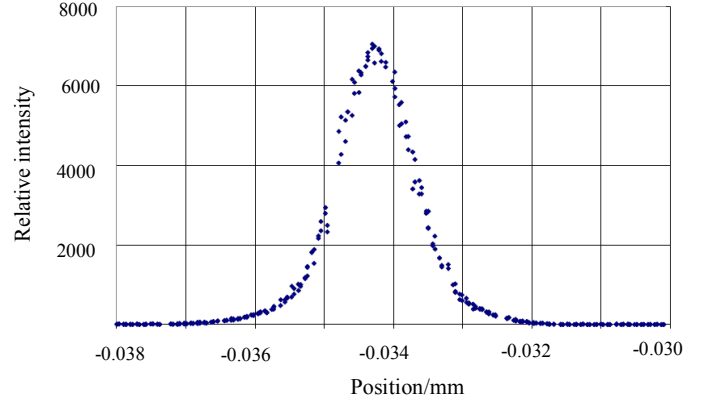


Fig. 5 The spread size of electrons in the silica substrate

### 4.2 PSF of MCP Image Intensifier

MCP image intensifier mainly consists of optical cathode, micro-channel plate (MCP) and fluorescence screen. MCP locates between the optical cathode and the fluorescence screen. MCP input plane is 0.1mm-0.3mm away from the optical cathode and the output plane is about 0.5mm~1.3mm away from the screen. Firstly, photoelectrons are excited from the cathode by incident beams. Then, driven by forward accelerating electric field between the cathode and the MCP input plane, electrons would be injected into the MCP input plane almost along a straight direction before being multiplied in micro-channels. Then they would be transmitted out of the MCP output plane and accelerated again by the electric field between the output plane and the screen. Finally, electrons would impact onto the screen to generate a corresponding fluorescence image.

Spatial resolution of the MCP image intensifier depends on multiple factors, various superposed voltages, exposure quantity of the optoelectronic cathode, manufacturing process, etc.. dispersion effect of electrons in the cathode and fluorescence screen would be another important factor to damage the spatial resolution. MCP image intensifier used in the experiment could provide a spatial resolution of more than 37lp/mm. And the PSF could be given as follows<sup>[4]</sup>:

$$PSF(r) = \exp[-(r/0.02)^2] \quad (5)$$

where:  $r$  stands for the radius (mm). The electron spread function of a typical MCP image intensifier is given in Figure 6. As shown in the figure, the diameter is about 0.06mm corresponding to 10% of PSF. Take account the minification factor of 1.5, and the spatial resolution of the MCP image intensifier is basically equal to that of the CCD camera.

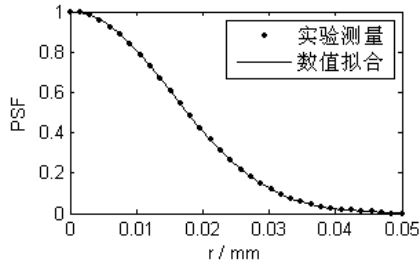


Fig. 6 The experimentally obtained electron spread function of the MCP image intensifier

### 4.3 Fluorescence Dispersion Effects

The fluorescence dispersion could be divided into two parts. One is the fluorescence dispersion in the scintillator; another one is due to the defocusing in the optical imaging system. Secondary electrons would be generated by interactions between  $\gamma$ -rays and the scintillator. And electrons would move within the scintillator and induce energy deposition. Part of this energy would be converted into fluorescent lights. Each of electron trajectories would be acting as a point light source. Due to the homogenous spatial distribution of lights, only some lights could be collected by the light collecting system, while most of them would be dispersed within the scintillator. During the dispersion, in the interface, half penetration half refraction and full reflection occur, while in the scintillator, only scattering takes place. The deliberately designed optical imaging system used in the experiment was made up of 12 lenses to provide a light collecting efficiency 30%. At the same time, defocusing effects induced by the fluorescence dispersion would also affect the spatial resolution.

Similarly, the edge method was again used to measure the fluorescence spatial resolution in the radiographic system. The spatial resolution of the fluorescence was calibrated on a pulsed X-rays source with energy of about 0.3 MeV. The distance between the scintillator and the radiation source was about 250 cm, and the spatial resolution of X-rays was presumably homogenous. In addition, effects of transmittance range of secondary electrons were neglected, which had been rationalized experimentally and theoretically. During the experiment, a 0.1 mm-thick copper film was tightly contacted with the scintillator surface, and the film was reasonably considered as the edge in the experiment. The SNR of the optical imaging system was finally found to be 10:1. After data processing, the MTF of the spatial resolution corresponding to 10% intensity was about 5 lp/mm (as shown in Figure 7), which was obtained with additional contributions from effects of the MCP image intensifier and the CCD device upon the fluorescence transmission.

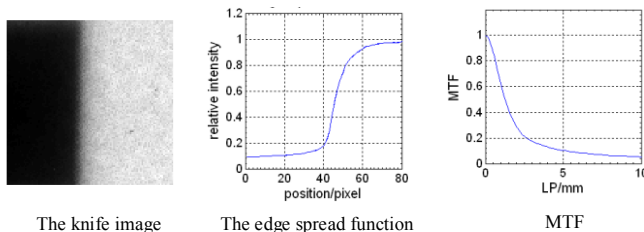


Fig.7 The spatial resolution of the fluorescence transmission in the system

### 4.4 Transmittance Range of Secondary Electrons in Scintillator

The spatial resolution of  $\gamma$ -rays in the scintillator crystal mainly depends on the transmittance range of secondary electrons and the fluorescence dispersion in the scintillator [13, 14]. Interactions between  $\gamma$ -rays and the scintillator would generate secondary electrons. Each would be a small light source, whose size would be decisive for the resolution limit. In order to get the fluorescence size of a single secondary electron, an optical imaging system with high light collecting efficiency was adopted in addition to a high sensitivity camera. Movement trajectories of secondary electrons were obtained.

The distance between the scintillator and the radiation source was 400 cm, the dose on the scintillator was  $3.7 \times 10^7 \text{ cm}^{-2} \cdot \text{s}^{-1}$  and a shading plate 30 mm in diameter was placed behind the scintillator to contain an effective image size within this range while exposure time was 0.1 ms. The fluorescence image is given in Figure 8. Miscellaneous speckle effects could be watched. Speckle images are in array distribution, no sign for linear propagation of electrons. This might attribute to the limit of the spatial resolution of the optical system and fluorescence dispersion effects in the scintillator and transmission system. Due to their effects, only degraded electron trajectories could be observed in the image.

With energy higher than 0.1 MeV, the ratios between energy depositions in the scintillator with luminescent efficiencies could be considered equal. Then for any speckle array, approximately, signal intensities over 50% higher than the peak would be classified as electron trajectories, whereas those below this level would be results of scattered fluorescence. According to the estimation of miscellaneous speckle sizes, the electron dispersion size is predictably 2 to 3 pixels, which, in dealing with the PSF of about 4 to 6 pixels, corresponds to a spread size of 0.4 mm to 0.6 mm size.

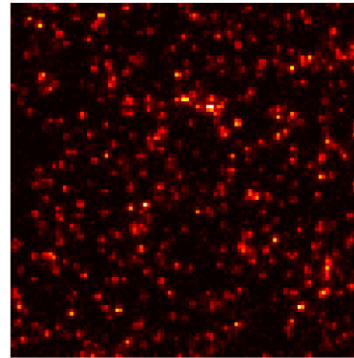


Fig.8 Speckle effects of secondary electrons in the scintillator

For a detailed description of the PSF of  $\gamma$ -rays in the scintillator, MCNP program was introduced to track and simulate the transportation process of  $\gamma$ -rays in the scintillator. And for the theoretical computation, the electronic fluorescence efficiency was supposed to be proportional to the electronic energy deposition efficiency [9,10]. Other conditions for the computation included the scintillator thickness (10 mm) and the interval of the radiuses of the concentric cylinders (0.010 mm). Energy disposition distributions in the scintillator were calculated for  $\gamma$ -rays respectively 0.3MeV and 1.25MeV in energy, whose results are given in Figure 9. As shown in the figure, the maximal

transmittance range of 0.3 MeV  $\gamma$ -rays on the projecting plane is about 0.2 mm, while the range increases to 0.8mm for 1.25 MeV rays. And the PSF sizes corresponding to the 1% intensity are 0.44 mm.

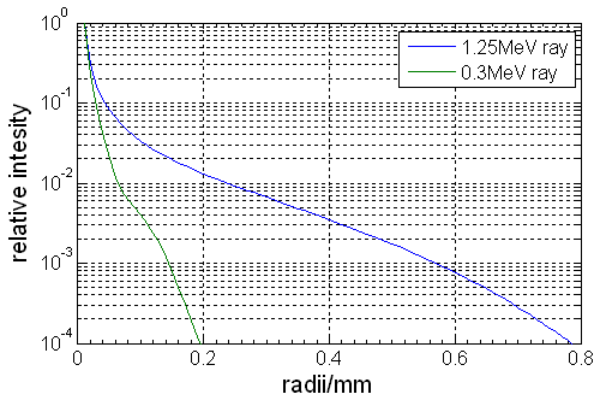


Fig. 9 The PSF of  $\gamma$ -rays in the scintillator

## 5 Conclusion

The spatial resolution of  $\gamma$ -rays camera was measured on a 1.25MeV source with edge method. Due to the relatively big DQE and quantum gain of gamma-rays, etc., the experimental data was processed by averaging multiple images and fitting curves. According to experimental results, the MTF (modulation transfer function) of spatial resolution at the 10% intensity was about 2 lp/mm. Based on this, further analysis was made for spatial resolutions of the MCP image intensifier and the CCD device. Besides, the spatial resolution of the scintillating fluorescence was measured as well as dispersion effects of secondary electrons in the scintillator. As results indicated, both fluorescence dispersion and dispersion of secondary electrons are major factors that affect the spatial resolution.

## Acknowledgements

The study presented in this paper is sponsored jointly by CAEP Sci. & Tech. Development Foundation (Contract No.: 2010B0103006 and 2011B0103017) and National Natural Science Foundation (Contract No.11005095). And the experimental study was made on the pulsed X-rays source in Northwest Institute of Nuclear Technology and with great help from Prof. Guo Jianming. Authors owe great gratitude to all of them.

## References

- [1] Scott Watson, Todd Kauppila, et al., "The High-Energy radiographic machine Emitting X-rays flash radiographic camera," SPIE, Vol.2869, P920-928.
- [2] George J. Yates, Nicholas S. P. King, "High-frame intensified fast optically shuttered TV cameras with selected imaging applications, SPIE Vol.2273, P126-149(1997).
- [3] P. B. Gree and T. van Doorn, "Evaluation of an algorithm for the assessment of the MTF using an edge method," Med Phys. Vol.27(9), P-20482059(2000).

- [4] Zhu Hongquan, "Study on the image restoration of Y-ray pinhole imaging system," Dissertation submitted to Tsinghua university in partial fulfillment of the requirement for the degree of Doctor of Engineering.
- [5] P. Z. Takacs and I.Kotov, "PSF and MTF measurement methods for thick CCD sensor characterization, Proc. of SPIE Vol.7742, p774207(2010).
- [6] Armin Karcher, Christopher J. Bebek, "Measurement of lateral charge diffusion in thick fully depleted, back-illuminated CCDs," IEEE transactions on nuclear science, Vol.51, No.5, p2231-2237(2004).
- [7] Horst Schwarzer, and Anko Boerner, "Dynamic PSF and MTF measurement on a 9k TDI CCD," Proc. of SPIE Vol.7106, p71061F(2008).
- [8] Zhu Hongquan, Wang Kuilu, MTF Measurement and analysis of Microchannel Plate Image Intensifiers, ACTA PHOTONICA SINICA, Vol. 36 No. 11, p1983-1986 (2007).
- [9] Ma Jiming, Wang Kuilu, Research on PSF of scintillator as  $\gamma$ -ray fluorescence image converter, Nuclear electronics & detection technology, Vol.31, No.4, p473-478(2011).
- [10] Zhu jinhui, Niu Shengli, Ma Jiming, "Energy deposition of gamma rays in LSO crystal, High power laser and particle beams," Vol.22, No.6, p1351-1354(2010).